Hindawi Publishing Corporation
Journal of Nanomaterials
Volume 2012, Article ID 283031, 8 pages
doi:10.1155/2012/283031

Research Article

Microstructure and Crystallization Kinetics of Polyurethane Thermoplastics Containing Trisilanol Isobutyl POSS

Vinicius Pistor,[1,2] Daniela de Conto,[1] Felipe Gustavo Ornaghi,[1,2] and Ademir José Zattera[1]

[1] *Laboratory of Polymers, Center of Exact Sciences and Technology (CCET), University of Caxias do Sul (UCS), 95070-560 Caxias do Sul, RS, Brazil*
[2] *Laboratory of Advanced Polymers, Federal University of Rio Grande do Sul (UFRGS), 91501-970 Porto Alegre, RS, Brazil*

Correspondence should be addressed to Ademir José Zattera, ajzattera@terra.com.br

Received 14 November 2011; Revised 24 January 2012; Accepted 28 February 2012

Academic Editor: Sérgio Henrique Pezzin

The synthesis of thermoplastic polyurethanes (TPU) from the reaction of a NCO group-containing prepolymer and 0, 1.14, 1.71, and 2.28 wt% of trisilanol isobutyl polyhedral oligomeric silsesquioxane (POSS) was carried out in an instrumented batch mixer. The samples were characterized by thermogravimetric analysis (TGA), differential scanning calorimetry (DSC), X-ray diffraction (XRD), and scanning electron microscopy (SEM). SEM analysis shows that the incorporation of POSS promoted strongly aggregation through physical interactions (formation of POSS-rich domains). Modifications in the TPU microstructure and the reduction in the crystal size were observed in the XRD diffractograms. The incorporation of POSS equally altered the TPU crystallization, and samples bearing higher concentrations of POSS formed two distinct types of crystalline structures. The kinetics of crystallization showed that nucleation strongly depends on the balance between TPU crystal formation and POSS-rich domains.

1. Introduction

Polyurethanes represent a class of polymers with wide applications, including the medical, automotive, and industrial sectors [1]. These materials are an important class of thermoplastic and thermosetting polymers because of their mechanical, thermal, and chemical properties, which can be defined through the proper selection of a huge variety of materials [2]. The characteristic structural element in the vast majority of polyurethanes is the urethane group, based on a polyaddition reaction. The urethane bonds result from the reaction of an isocyanate (–N=C=O) with an alcohol (−OH) group [1, 3]. The application of polyurethane elastomers with thermoplastic features was first described in the 1950s, and they were first marketed in the 1960s. Currently, thermoplastic polyurethane (TPU) is one of the most versatile products within the group of engineered thermoplastics with elastomeric properties [4].

According to Odian [5], thermoplastic elastomers are multifunctional polymeric materials that usually present the processability of thermoplastics and the elasticity of vulcanised elastomers. However, some aspects of these materials restrict some of their applications even today because of the peculiarities of their processing. For example, when processing TPU by mixing in the molten state, they become extremely susceptible to thermal degradation and thermooxidation in the range of temperatures required for processing [6].

Polyurethanes are generally characterised by their low-thermal stability due to the thermally unstable urethane group. The thermal decomposition of urethane starts at the range from 150 to 200°C [7]. Above the temperatures of thermal stability, the urethane bonds dissociate and reassociate simultaneously [8]. The degradation caused by the dissociation of urethane bonds is reversible; however, since reduction in temperature leads to a recovery of urethane (reaction between the hydroxyl and the terminal isocyanate) [9–11], Lu et al. [12] described that the thermal degradation of polyurethanes in the melt state is inevitable as a result of the fusion that usually occurs around or above the temperature for stability of the urethane bonds (temperatures lower than 250°C). As a result of the process

of dissociation and reassociation of urethane, the molecular weight can change. Therefore, heat treatment of thermoplastic polyurethane above a critical temperature, particularly under experimental conditions or during processing in the molten state, can significantly change the viscosity, the crystallization behaviour, and even the mechanical properties of the resulting liquid [8]. Fortunately, with the rise of nanotechnology as one of the most promising fields in the development and modification of polymeric materials, many materials previously found to be too difficult to process can be revisited.

Polyhedral oligomeric silsesquioxane (POSS) molecules are structurally well defined as a three-dimensional cage [13, 14]. These compounds bear a silicon-containing inorganic core surrounded by organic groups. The typical size of the POSS cages is approximately 1.5 nm. Because of its hybrid nature and nanometric size, POSS are promising materials for nanocomposites [13–16]. The incorporation of POSS cages into the main chain of polymers can result in drastic changes in their properties, including increased processing temperature, oxidation resistance, surface hardness, improved mechanical properties, and reduced flammability and heat release. These improvements have been observed for a large number of thermoplastic polymers and some thermosetting polymers [13]. Aiming to improve the thermal stability of TPU in the range from 150 to 200°C [7] associated with the crystallization process, *in situ* addition of the trisilanol isobutyl polyhedral oligomer silsesquioxane (POSS) into the synthesis of thermoplastic polyurethane was achieved through a torque rheometer. Measurements were then carried out to evaluate the changes in thermal and morphological properties generated in the crystal structure of these nanocomposites.

2. Materials

The materials used in this study were Urecon 185 prepolymer (18% free NCO Coim), 1,4-butanediol (BDO, MCassab), and polyhedral oligomer trisilanol isobutyl silsesquioxane (POSS) (POSS, Hybrid Plastics). These materials were used as received. The chemical structures of the materials are illustrated in Figure 1.

3. Methods

3.1. Synthesis in Torque Rheometer. The syntheses were performed in an instrumented torque rheometer using roller type rotors counter-rotating at 90 rpm and at a temperature of 70°C for 60 minutes. The total volume of the rheometer chamber is 75 cm^{-3}, the total mass of each mixture being 50 g. The stoichiometry was calculated on the basis of the equivalents of isocyanate (NCO) and hydroxyl (OH) groups for the prepolymer and BDO, respectively (molar ratio NCO/OH = 1/1). A rate of 98% reacted NCO was maintained throughout the syntheses. Amounts of 1.14, 1.71, and 2.28 wt% of POSS were added *in situ* to the TPU synthesis reaction. The polymers were removed from the rheometer as solids and postcured at 90°C for 24 hours.

3.2. Thermogravimetric Analysis (TGA). The TGA analysis (TGA50-Shimdzu) was performed under an N_2 atmosphere (50 mL·min^{-1}) using approximately 20 mg of each sample. The analysis was performed at a heating rate of 10°C·min^{-1} from 25 to 730°C.

3.3. Differential Scanning Calorimetry (DSC). The DSC analysis (DSC 50-Shimadzu) was performed under a N_2 atmosphere (50 mL·min^{-1}) using approximately 10 mg of each sample. Samples were initially heated from ambient temperature to 250°C at a heating rate of 10°C·min^{-1}, cooling until the temperature of −80°C and then heated again at a rate of 10°C·min^{-1} to 250°C.

3.4. X-Ray Diffraction (XRD). X-ray diffractograms were collected using a sample holder mounted on a Shimadzu diffractometer (XRD-6000) with monochromatic CuKα radiation (λ = 0.15418 nm) and the generator working at 40 kV and 30 mA. Intensities were measured in the range of $3 < 2\theta < 35°$, typically with scan steps of 0.05° and 2 s/step (1.5° min^{-1}). Peak separations were carried out using Gaussian deconvolution. The determination coefficients (r^2) were close to unity (0.9982 and 0.9991). The d spacings were calculated using the Bragg equation [17, 18], and the crystallite sizes (L) were calculated using the Scherrer equation [17, 18].

3.5. Scanning Electron Microscopy (SEM). Scanning electron microscopy (SEM) was carried out using a Superscan S-550 instrument with a secondary electron detector and an acceleration voltage of 15.0 kW. The scanning was carried out at a magnification of 200 × (50 μm) and 1200 × (10 μm). The samples were previously covered with gold.

3.6. The Avrami Method. Throughout the decades, several kinetic models were developed to quantify the kinetic parameters involved in solid state reactions. For example, the original derivation performed by Avrami [19–21] was simplified by Meares [22] and Hay [23]. Equation (1) represents the original derivation Avrami used for isothermal experiments. Equation (2) presents the double logarithm used to obtain the kinetic parameters proposed by Avrami:

$$\alpha(t) = 1 - e^{-kt^n}, \tag{1}$$

$$\ln[-\ln(1-\alpha(t))] = \ln k + n \ln t, \tag{2}$$

where k is the Avrami constant dependent on the rate of nucleation or crystal growth and n is the Avrami exponent dependent on the dimensional process.

Taking into account the influence of the rate of heating/cooling on nonisothermal crystallization on the parameter k, Jeziorny [24] proposed the following relation using the Avrami equation:

$$\ln k' = \left(\frac{\ln k}{\phi}\right), \tag{3}$$

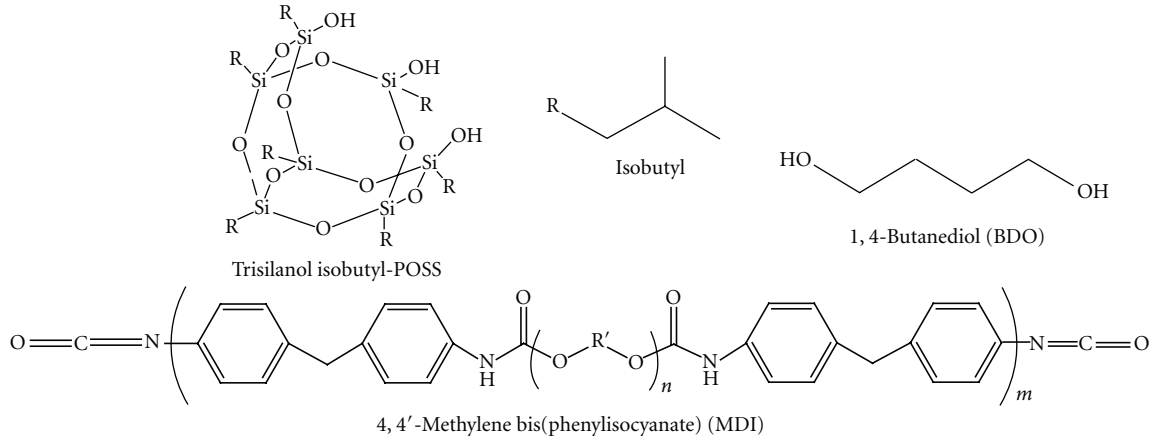

Figure 1: Chemical structures used for obtaining the nanocomposites studied.

where ϕ is the heating rate in $^{\circ}C \cdot min^{-1}$. Through the analysis of Jeziorny, in this case α is a function of temperature ($\alpha(T)$). Therefore, the constant k' was corrected as a function of ϕ.

4. Results and Discussion

4.1. Morphologic Characteristics. Figure 2 shows images obtained by cryogenic fracture in scanning electron microscopy (SEM) at ×200 and ×1200 related to images I and II, respectively. The images (a), (b), (c) and (d) correspond to 0, 1.14, 1.71 and 2.28 wt% of POSS, respectively. The morphology of the TPU presents detachment regions at interfacial fractures [25]. The incorporation of POSS nanocages (images Ib, Ic and Id) changed the morphology and showed more detachment regions than those observed for pure TPU. This modification in the microstructure was more evident by observing images IIa, IIb, IIc and IId. The POSS incorporated *in situ* in the TPU reaction was dispersed as clusters with diameters from 1 to 3 μm throughout the TPU microstructure.

This dispersion occurred because POSS has a strong aggregation effect through physical interactions [26]. This strong aggregation effect may be due to the silicon and oxygen cage being hydrophobic, as well as the isobutyl branches having poor chemical interactions with the TPU, which is hydrophilic in character. In this way, the only face of the nanocages interacting with the matrix would be the hydroxyls on the open face of the POSS cage (Figure 1).

4.2. X-Ray Diffraction (XRD). Three diffraction peaks in the range $2\theta = 18 - 23^{\circ}$ can be noted in Figure 3. These diffraction peaks with interplanar spacing (d-spacing) of 0.463, 0.413, and 0.379 nm were related to the lateral distances in the contours (interfaces) of the hard crystallised segments [27, 28]. These diffraction peaks were superimposed on the amorphous halo (Figure 3(b)) for the dispersion of TPU chains with regular interplanar spacing [29]. The hard segments of the crystal were related to various hydrogen bonds between urethane groups [30].

In the range of reflection of $2\theta \approx 11^{\circ}$, the diffraction peaks corresponding to a d-spacing of 0.851 nm were associated with the reflections reminiscent of the plan (001) and related to the perpendicular region of the lamellar surface [28]. The presence of POSS was confirmed in the scanning range of $2\theta = 7 - 8^{\circ}$ with d-spacing of 1.2 and 1.1 nm for peak V and VI, respectively [31]. Through the calculation of the crystallite size by the Scherrer equation [17, 18], it was possible to evaluate the influence of POSS domains in the crystalline structure of the TPU. The determination of the crystal size is detailed in Table 1.

The diffraction peaks of V and VI were associated with the microphase separation of the crystalline structure of POSS [31]. The incorporation of POSS reduced both the crystallite size (L_I) of the region perpendicular to the lamellar surface [28] and L_{II}. For the sizes L_{III} and L_{IV}, there was no clear tendency related to the incorporation of POSS, but all POSS-containing samples showed reduced L_{IV} compared with pure TPU. As the sizes of crystals in the region between $2\theta = 18 - 23^{\circ}$ were related to the formation of spherulites [32], the reduction in size of the crystals and the perpendicular region to the lamellar surface showed that the presence of POSS microdomains promoted modifications in crystal formation. Moreover, the larger the amount of POSS incorporated, the smaller the size of the POSS crystalline domains (L_V and L_{VI} in Table 1) and, consequently, the smaller the crystalline domains formed between the TPU hard segments (L_I and L_{II} in Table 1).

4.3. Crystallization Behavior by the Avrami Method. Considering the effects of the incorporation of POSS in the crystal structure of the TPU, it was possible to verify through the crystallization thermograms in Figure 4 that the addition of 1.14 wt% of POSS increased the TPU crystallization temperature.

This observation suggests that the crystallization was negatively impacted by nucleation through the POSS microdomains (Figure 2). The samples containing 1.71 and 2.28 wt% of POSS had even a higher range of crystallization temperature than the sample containing 1.14 wt% and

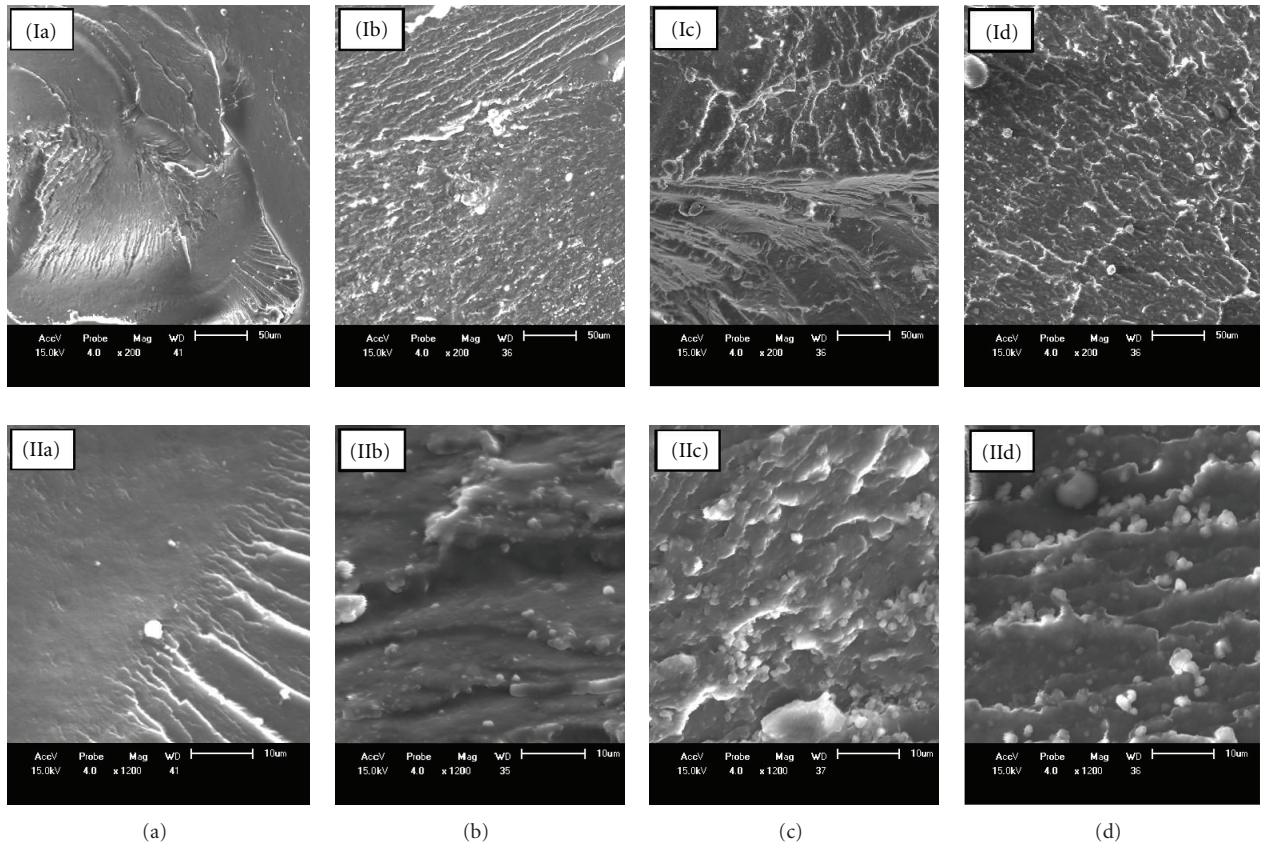

Figure 2: (a), (b), (c), and (d) morphological images obtained by scanning electron microscopy (SEM) for TPU and the TPU/POSS systems studied corresponding to 0, 1.14, 1.71, and 2.28 wt% of POSS at magnifications of ×200 and ×1200 for I and II, respectively.

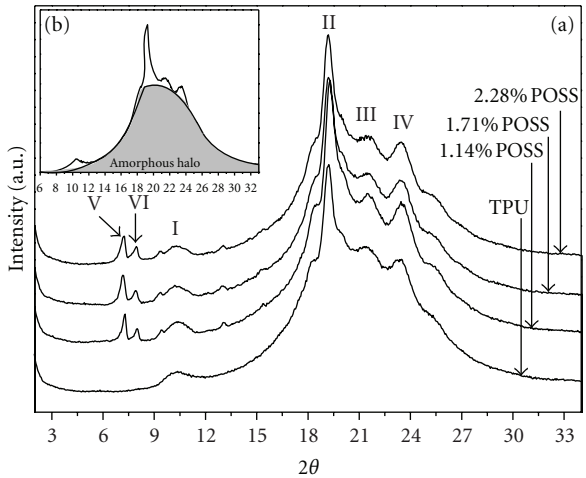

Figure 3: Analysis of X-ray diffraction data obtained with scan steps of 0.05° and 2 s/step (1.5° min^{-1}) for the samples studied where (a) Comparative curves obtained for the nanocomposites and (b) representation of an amorphous halo in the TPU sample.

showed a double crystallization peak that indicated the formation of two distinct types of crystalline structures.

The sample containing 1.14 wt% did not cause the same effect probably due to the fact that the amount of POSS seen in the SEM analysis (Figure 2) is not sufficient to modify the crystallization.

Table 1: Crystallite sizes obtained by the Sherrer equation for the diffraction peaks studied.

Sample	L_{I} (nm)	L_{II} (nm)	L_{III} (nm)	L_{IV}(nm)	L_{V} (nm)	L_{VI} (nm)
TPU	148.27	21.07	123.42	96.24	—	—
1.14%	30.37	20.49	127.79	60.78	54.49	162.35
1.71%	21.24	18.31	94.04	53.79	68.44	126.11
2.28%	16.73	17.27	135.38	58.57	22.99	107.85

The Avrami method was used to determine the kinetic parameters of crystallization at a heating rate of 10°C·min^{-1}. By integrating the exothermic crystallization peaks observed in Figure 4 it was possible to determine the conversion for the samples studied using the following relationship:

$$\alpha = \frac{1}{\Delta H_c} \int_0^t \frac{d(\Delta H_t)}{dt} dt, \tag{4}$$

where α is the fraction converted at time t, ΔH_c is the total heat involved in the process of crystallization, and ΔH_t is the heat generated at each time instant (t) [33, 34].

The conversion (α) curves in Figure 5 represent the evolution of the crystallization process, and as observed in the DSC thermograms, it was noted that the samples containing

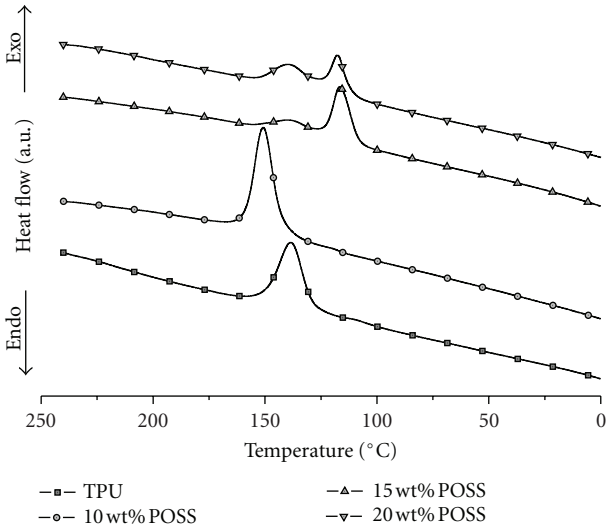

Figure 4: Crystallization thermograms obtained at a cooling rate of $10^{\circ}C \cdot min^{-1}$ after removal of the thermal history carried out at a heating rate of $10^{\circ}C \cdot min^{-1}$ from -50 to $240^{\circ}C$.

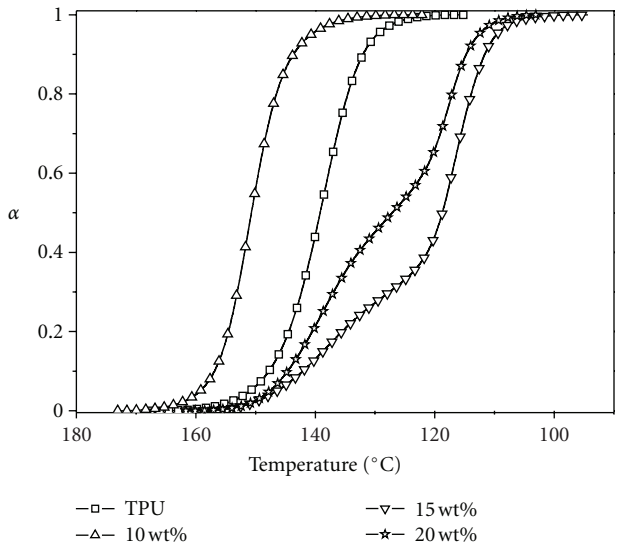

Figure 5: Conversion (α) curves obtained by integrating the exothermic peak crystallization.

1.71 and 2.28 wt% of POSS presented two velocity crystallization gradients. These two ranges of crystallization will be discussed as the first and second stages of crystallization in these samples. With the determination of α and making use of (2), Figure 6 representing the adjustment made to the Avrami equation was obtained [19–21].

According to Liu et al. [35], the Avrami equation represents only the initial polymer crystallization growth steps. The spherulites grew outward with a constant radial growth rate until a shock occurred as a result of the end of growth at the intersection of the crystals. Thus, the region for obtaining kinetic parameters related to the linear fit was determined at the more linear region in Figure 6. Table 2 presents the results obtained from DSC thermograms and the Avrami model. The degree of crystallinity calculated from the DSC analysis was determined by considering the enthalpy of crystallization of a 100% crystalline material ($H_{100\%}$ = 196.8 $J \cdot g^{-1}$) [34].

From the results depicted in Table 2 it was possible to observe a crystallization shift to higher temperatures for the sample containing 1.14 wt% of POSS. Moreover, the samples containing 1.71 and 2.28 wt% presented decreased enthalpy and degree of crystallinity, respectively. The reduction in ΔH_c and degree of crystallinity (% Cryst.) in the samples containing 1.71 and 2.28 wt% were associated with higher dispersion of the POSS compared with the sample containing 1.14 wt%. The 1.14 wt% sample had higher ΔH_c. This probably occurs because at this POSS content, the effect of spatial restriction at crystal interfaces is reduced. This would explain the increase in the crystallization temperature and crystallinity degree. It was also observed (L_{VI} in Table 1) that the incorporation of a higher nanocage content promotes a reduction in the POSS microphase sizes. The presence of POSS microdomains favoured the interaction of rigid segments with the POSS nanocages through the effect of

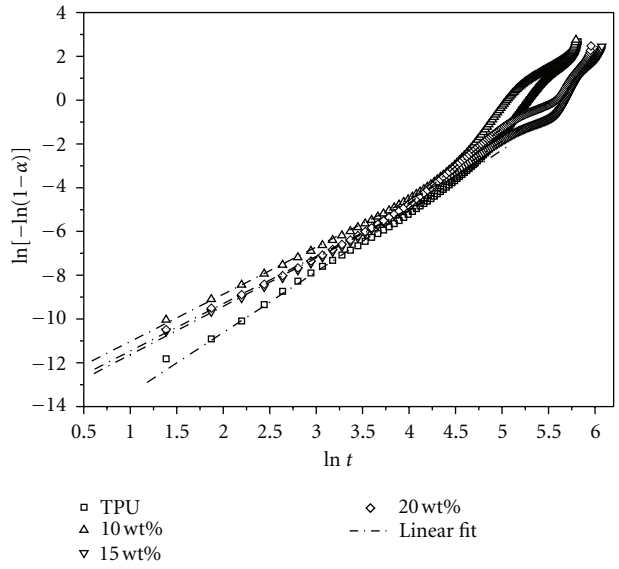

Figure 6: Linear fit used to obtain the Avrami kinetic parameters.

space hindrance at the interface of crystal growth as compared with pure TPU. This observation was supported by a double crystallization peak, which suggests that these samples were undergoing distinct nucleation and crystal growth phenomena.

The value of the rate constant (k'), corroborated with the results observed in the crystallization thermograms. With the increase in POSS content, the constant velocity of crystal growth and the half-life ($t_{1/2}$; i.e., the time required for 50% of the crystallization to occur) for the first crystallization stage decreased. The half-life reduction could be associated with the fact that smaller crystals were forming in the presence of POSS; thus, even with reduced k' the lowest

Table 2: DSC and kinetic crystallisation parameters for the Avrami method obtained at a heating rate of $10^{\circ}C \cdot min^{-1}$.

Sample	T_c (°C)	ΔH_c ($J \cdot g^{-1}$)	% Cryst.	k' (min^{-1})	$t_{1/2}$ (min)	n	r
TPU	138.54	24.02	12.21	16.18	0.32	2.77895	0.9986
1.14 wt.%	150.84	28.36	14.41	13.18	0.26	2.15848	0.9988
1.71 wt.%	140.2 and 115.9	19.68	10.00	13.88 and 16.00	0.26 and 0.33	2.21 and 2.83	0.9975
2.28 wt.%	140.8 and 117.9	18.82	9.56	13.62 and 18.77	0.25 and 0.39	2.16 and 3.50	0.9992

values of $t_{1/2}$ were principally dependent on the size of the crystalline domains and the type of crystal formed. The Avrami exponent (n) values were found to be $n \approx 3$ for pure TPU. The effect on the crystallization here described by the Avrami method would be that crystallization is controlled by three-dimensional diffusion in the form of spheres (spherulites) [22], characteristic of the type of crystals formed in the TPU crystallization [24, 32].

Begenir et al. [36], studying the crystallization behaviour of polyurethane elastomeric copolymers and polyether-b-amide, observed that the crystallization occurred in three dimensions from precores of hard segments due to regions of microphase separation (crystalline and amorphous). The authors also described that crystallization occurred through the association of hard segments by hydrogen bonding between urethane groups. Table 2 shows that by adding POSS (considering only the first stage of crystallization of the samples containing 1.71 and 2.28 wt%), the Avrami exponent values found were $n \approx 2$. The exponent n tending to 2 indicates that the crystallization could occur sporadically as two-dimensional discs [22]. This change in the values of n is in agreement with the reduction in crystal sizes L_{I} and L_{II} in Table 1. Then, for the second crystallization stage observed for samples containing 1.71 and 2.28 wt% of POSS, the values of k', $t_{1/2}$, and n were similar to those of pure TPU. The values of k', $t_{1/2}$ in the second crystallization stage (for 1.71 and 2.28 wt% of POSS) demonstrate as seen earlier the formation of radial spherulites. The sample containing 1.14 wt% of POSS showed only one value of $n \approx 2$, and the formation of disks could increase crystal packing. This assumption would explain why higher values were observed for %Cryst. and ΔH_c for the sample containing 1.14 wt% of POSS.

Figure 7 illustrates the crystallization behaviour related to the results shown in Table 2. For the exponent $n \approx 3$ (pure TPU), the dimensional processes demonstrated that crystal growth occurred radially along with the formation of small cores until the formation of well-defined crystals. The spherulites were composed of lamellar structures, which grow out radially. The individual chains were folded back and tangentially to the spherical surface of the growing spherulites [37]. However, at 1.14 wt% of POSS, the Avrami exponent tended to $n \approx 2$. This result shows that POSS impeded the radial crystal growth, thus making crystals oriented in at least one dimension of the plane. This behaviour corroborated the reduction in L_{I} displayed in Table 1.

According to Sperling [38], the crystal growth rate in the radial direction is constant until spherulites are formed. However, impurities, such as atactic components, can become a hindrance at the interlayer region. According to Zheng et al. [39], POSS tends to crystallise in two-dimensional lamellar structures. Although lamellar structures are found in low amounts of POSS, the plates became more organised for increased amounts of POSS. Strachota et al. [26] described the POSS undergoing strong aggregation due to physical interactions. As the nanocages interact strongly with each other [26] and tend to crystallise in two dimensions to form lamellar structures [39], it was possible to rationalize why the Avrami exponent tended to $n \approx 2$ for the TPU crystallization in the presence of POSS.

For the samples containing 1.71 and 2.28 wt% of POSS, two stages of crystallization were observed (Figure 7). The first crystallization stage was typical of disk formation with $n \approx 2$ due to the effect of nucleation on POSS, which acted as a system impurity. In the second crystallization stage, the change in the Avrami exponent (n) from 2 to 3 suggests that after the formation of crystals in the form of discs, spherulites formed.

This second stage was possibly related to the dispersion of the nanocages and the POSS crystalline domains reduction in size as determined by XRD. Moreover, since both the ΔH_c and the percentage of crystallinity (%Cryst.) suggested the formation of smaller crystals, the higher heterogeneity in the formation of the two crystalline phases was ascertained.

5. Conclusions

The influence of isobutyl trisilanol POSS on the crystalline structure of thermoplastic polyurethane was studied. POSS was added to replace the percentage mass of 1.4 butanediol in the *in situ* synthesis reaction by a torque rheometer.

The incorporation of POSS showed that clusters along the TPU microstructure occurred as a result of a strong aggregation effect through physical interactions between the nanocages.

The POSS reduced crystallite sizes were associated with spherulites formation at the crystallographic plane L_I and at the interlayer region of the crystals L_{II}. Increased POSS percentages also entrained diminished microdomains (L_{VI}) size.

The crystallization temperature was increased for the 1.14 wt% of POSS sample. However, for 1.71 and 2.28 wt% of POSS in the system, a double crystallization peak was noted, indicating the formation of two distinct types of crystalline structures. The adverse behaviour observed for the sample containing 1.14 wt% of POSS was associated to the low level of the nanocages incorporation. The double crystallization peak for the 1.71 and 2.28 wt% of POSS samples occurs probably because of the reduction in crystal size at the L_{I} and L_{II} planes in XRD analysis and by the spatial hindrance caused at the crystal interface.

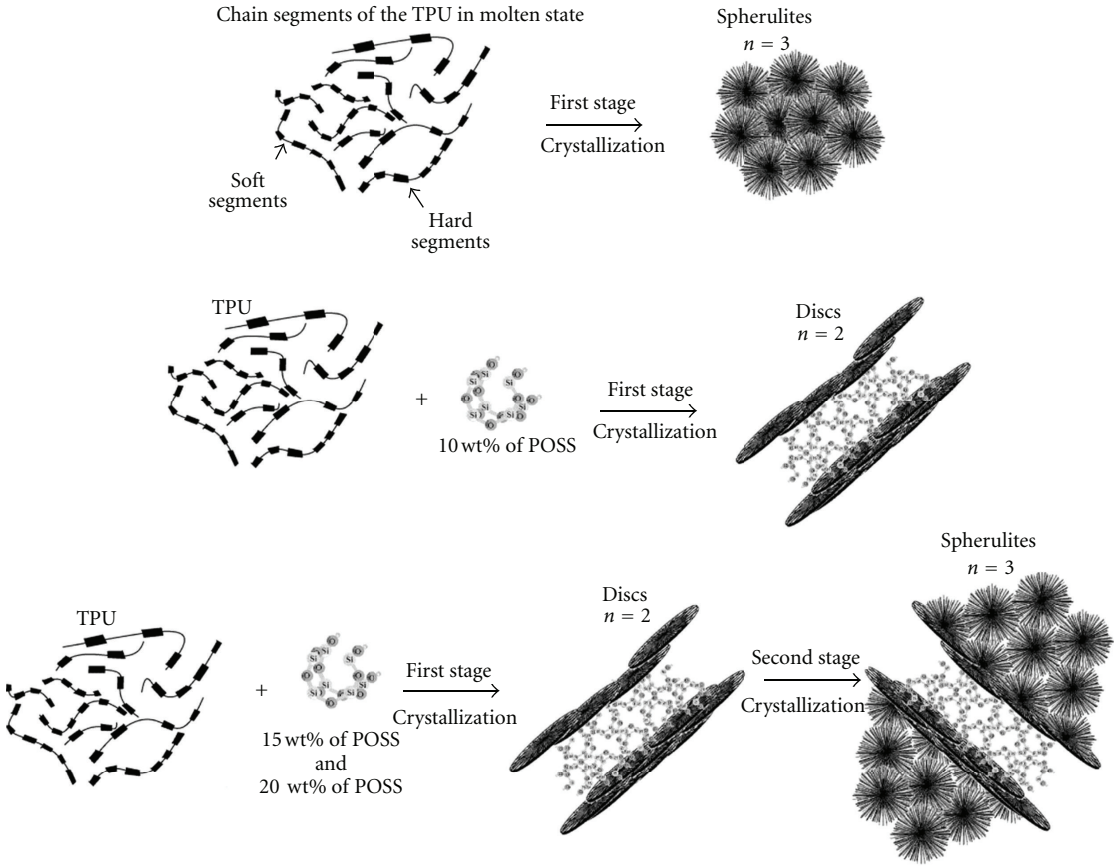

Figure 7: Schematics for the TPU and the nanocomposites nucleation and crystal growth phenomena.

The rate of crystal growth and the reduction in half-lives with increasing POSS content in the first crystallization stage was likely associated with the formation of smaller crystals in the presence of POSS. In the presence of POSS, crystallization occurs as two-dimensional discs, forming lamellar structures. The samples containing 1.71 and 2.28 wt% of POSS showed two crystallization stages, forming disks at first and then moving to spherulites. These results suggest that even the formation of clusters upon POSS incorporation showed a strong influence on the crystal nucleation and growth mechanism and these modifications should be considered for future applications of this type of nanoparticles.

Acknowledgment

The authors gratefully acknowledge the Brazilian National Council for Scientific and Technological Development (CNPq) for financial support.

References

[1] G. T. Howard, "Biodegradation of polyurethane: a review," *International Biodeterioration & Biodegradation*, vol. 49, no. 4, pp. 245–252, 2002.

[2] C. R. Kumar and J. Karger-Kocsis, "Curing and mechanical behavior of carboxylated NBR containing hygrothermally decomposed polyurethane," *European Polymer Journal*, vol. 38, no. 11, pp. 2231–2237, 2002.

[3] C. A. Harper and E. M. Petrie, *Plastics Materials and Processes: A Concise Encyclopedia*, John Wiley & Sons, Hoboken, NJ, USA, 2003.

[4] J. Scheirs, "Historical overview of styrenic polymers," in *Modern Styrenic Polymers*, J. Scheirs and D. Priddy, Eds., John Wiley & Sons, West Sussex, UK, 2003.

[5] G. Odian, *Principle of Polymerization*, John Wiley & Sons, Hoboken, NJ, USA, 4th edition, 2004.

[6] B. Finnigan, D. Martin, P. Halley, R. Truss, and K. Campbell, "Morphology and properties of thermoplastic polyurethane nanocomposites incorporating hydrophilic layered silicates," *Polymer*, vol. 45, no. 7, pp. 2249–2260, 2004.

[7] P. R. Nair, C. P. R. Nair, and D. J. Francis, "Phosphazene-modified polyurethanes: synthesis, mechanical and thermal characteristics," *European Polymer Journal*, vol. 32, no. 12, pp. 1415–1420, 1996.

[8] T. Hentschel and H. Münstedt, "Kinetics of the molar mass decrease in a polyurethane melt: a rheological study," *Polymer*, vol. 42, no. 7, pp. 3195–3203, 2001.

[9] M. S. Sánchez-Adsuar, "Influence of the composition on the crystallinity and adhesion properties of thermoplastic polyurethane elastomers," *International Journal of Adhesion and Adhesives*, vol. 20, no. 4, pp. 291–298, 2000.

[10] A. Frick and A. Rochman, "Characterization of TPU-elastomers by thermal analysis (DSC)," *Polymer Testing*, vol. 23, no. 4, pp. 413–417, 2004.

[11] M. Van der Schuur, B. Noordover, and R. J. Gaymans, "Polyurethane elastomers with amide chain extenders of uniform length," *Polymer*, vol. 47, no. 4, pp. 1091–1100, 2006.

[12] Q. W. Lu, M. E. Hernandez-Hernandez, and C. W. Macosko, "Explaining the abnormally high flow activation energy of thermoplastic polyurethanes," *Polymer*, vol. 44, no. 11, pp. 3309–3318, 2003.

[13] L. Liu, M. Tian, W. Zhang, L. Zhang, and J. E. Mark, "Crystallization and morphology study of polyhedral oligomeric silsesquioxane (POSS)/polysiloxane elastomer composites prepared by melt blending," *Polymer*, vol. 48, no. 11, pp. 3201–3212, 2007.

[14] S. Bizet, J. Galy, and J. F. Gérard, "Molecular dynamics simulation of organic-inorganic copolymers based on methacryl-POSS and methyl methacrylate," *Polymer*, vol. 47, no. 24, pp. 8219–8227, 2006.

[15] Y. Liu, S. Zheng, and K. Nie, "Epoxy nanocomposites with octa(propylglycidyl ether) polyhedral oligomeric silsesquioxane," *Polymer*, vol. 46, no. 25, pp. 12016–12025, 2005.

[16] A. Strachota, P. Whelan, J. Kriz et al., "Formation of nanostructured epoxy networks containing polyhedral oligomeric silsesquioxane (POSS) blocks," *Polymer*, vol. 48, no. 11, pp. 3041–3058, 2007.

[17] M. Wada and T. Okano, "Localization of Iα and Iβ phases in algal cellulose revealed by acid treatments," *Cellulose*, vol. 8, no. 3, pp. 183–188, 2001.

[18] U. J. Kim, S. H. Eom, and M. Wada, "Thermal decomposition of native cellulose: influence on crystallite size," *Polymer Degradation and Stability*, vol. 95, no. 5, pp. 778–781, 2010.

[19] M. Avrami, "Kinetics of change. I," *Journal of Chemical Physics*, vol. 7, no. 12, pp. 1103–1113, 1939.

[20] M. Avrami, "Kinetics of phase change. II Transformation-time relations for random distribution of nuclei," *Journal of Chemical Physics*, vol. 8, no. 2, pp. 212–224, 1940.

[21] M. Avrami, "Kinetics of phase change. III granulation, phase change, and microstructure," *Journal of Chemical Physics*, vol. 9, no. 2, pp. 177–184, 1941.

[22] P. Meares, *Polymers: Structure and Bulk Properties*, Van Nostrand, New York, NY, USA, 1965.

[23] J. N. Hay, "Application of the modified avrami equations to polymer crystallisation kinetics," *British Polymer Journal*, vol. 3, no. 2, pp. 74–82, 1971.

[24] A. Jeziorny, "Parameters characterizing the kinetics of the non-isothermal crystallization of poly(ethylene terephthalate) determined by d.s.c.," *Polymer*, vol. 19, no. 10, pp. 1142–1144, 1978.

[25] L. Pizzatto, A. Lizot, R. Fiorio et al., "Synthesis and characterization of thermoplastic polyurethane/nanoclay composites," *Materials Science and Engineering C*, vol. 29, no. 2, pp. 474–478, 2009.

[26] A. Strachota, I. Kroutilová, J. Kovárová, and L. Matejka, "Epoxy networks reinforced with polyhedral oligomeric silsesquioxanes (POSS). Thermomechanical properties," *Macromolecules*, vol. 37, no. 25, pp. 9457–9464, 2004.

[27] A. K. Nanda, D. A. Wicks, S. A. Madbouly, and J. U. Otaigbe, "Nanostructured polyurethane/POSS hybrid aqueous dispersions prepared by homogeneous solution polymerization," *Macromolecules*, vol. 39, no. 20, pp. 7037–7043, 2006.

[28] R. Androsh, J. Blackwell, S. N. Chvalun, G. Festel, and C. D. Eisenbach, "X-ray investigation of the structure of polyurethane elastomers based on 1,5-naphthalene diisocyanate," *Acta Polymerica*, vol. 48, pp. 363–368, 1997.

[29] G. Trovati, E. A. Sanches, S. C. Neto, Y. P. Mascarenhas, and G. O. Chierice, "Characterization of polyurethane resins by FTIR, TGA, and XRD," *Journal of Applied Polymer Science*, vol. 115, no. 1, pp. 263–268, 2010.

[30] L. Wang and Y. Wei, "Effect of soft segment length on properties of fluorinated polyurethanes," *Colloids and Surfaces B*, vol. 41, no. 4, pp. 249–255, 2005.

[31] J. Wu, Q. Ge, K. A. Burke, and P. T. Mather, "Crystallization of POSS in a PEG-based multiblock polyurethane: toward a hybrid hydrogel," *Materials Research Society*, vol. 847, pp. EE10.2.1–EE10.2.6, 2005.

[32] J. T. Koberstein and T. P. Russell, "Simultaneous SAXS-DSC study of multiple endothermic behavior in polyether-based polyurethane block copolymers," *Macromolecules*, vol. 19, no. 3, pp. 714–720, 1986.

[33] T. A. Ozawa, "A new method of quantitative differential thermal analysis," *Bulletin of the Chemical Society of Japan*, vol. 39, pp. 2071–2085, 1966.

[34] Y. Zhu, J. Hu, K. Choi, K. Yeung, Q. Meng, and S. Chen, "Crystallization and melting behavior of the crystalline soft segment in a shape-memory polyurethane ionomer," *Journal of Applied Polymer Science*, vol. 107, no. 1, pp. 599–609, 2008.

[35] W. Liu, H. Yang, B. S. Hsiao, R. S. Stein, S. Liu, and B. Huang, "Real-time crystallization and melting study of ethylene-based copolymers by SAXS, WAXD, and DSC techniques," *ACS Symposium Series*, vol. 739, chapter 12, pp. 187–200, 1999.

[36] A. Begenir, S. Michielsen, and B. Pourdeyhimi, "Crystallization behavior of elastomeric block copolymers: thermoplastic polyurethane and polyether-block-amide," *Journal of Applied Polymer Science*, vol. 111, no. 3, pp. 1246–1256, 2009.

[37] H. D. Keith and F. J. Padden, "Spherulitic crystallization from the melt. I. Fractionation and impurity segregation and their influence on crystalline morphology," *Journal of Applied Physics*, vol. 35, no. 4, pp. 1270–1285, 1964.

[38] L. H. Sperling, *Introduction to Physical Polymer Science*, John Wiley & Sons, New York, NY, USA, 2006.

[39] L. Zheng, S. Hong, G. Cardoen, E. Burgaz, S. P. Gido, and E. B. Coughlin, "Polymer nanocomposites through controlled self-assembly of cubic silsesquioxane scaffolds," *Macromolecules*, vol. 37, no. 23, pp. 8606–8611, 2004.